Mass dependence of pseudoscalar meson elastic form factors

Muyang Chen, Minghui Ding, Lei Chang, and Craig D. Roberts

Phys. Rev. D **98**, 091505 — Published 29 November 2018

DOI: 10.1103/PhysRevD.98.091505

Mass-dependence of pseudoscalar meson elastic form factors

Muyang Chen,[1] Minghui Ding,[1,2] Lei Chang,[1,*] and Craig D. Roberts[2,†]

[1] *School of Physics, Nankai University, Tianjin 300071, China*
[2] *Physics Division, Argonne National Laboratory, Argonne, Illinois 60439, USA*

(Dated: 23 October 2018)

A continuum approach to quark-antiquark bound-states is used to determine the electromagnetic form factors of pion-like mesons with masses $m_{0^-}/\mathrm{GeV} = 0.14, 0.47, 0.69, 0.83$ on a spacelike domain that extends to $Q^2 \lesssim 10\,\mathrm{GeV}^2$. The results enable direct comparisons with contemporary lattice-QCD calculations of heavy-pion form factors at large values of momentum transfer and aid in understanding them. They also reveal, *inter alia*, that the form factor of the physical pion provides the best opportunity for verification of the factorised hard-scattering formula relevant to this class of exclusive processes and that this capacity diminishes steadily as the meson mass increases.

1. Introduction. Perturbation theory in quantum chromodynamics [QCD] is applicable to hard exclusive processes; and for almost forty years the leading-order factorised result for the electromagnetic form factor of a pseudoscalar meson has excited experimental and theoretical interest. Namely [1–4], $\exists\, Q_0 > \Lambda_{\rm QCD}$ such that

$$Q^2 F_{0^-}(Q^2) \overset{Q^2>Q_0^2}{\approx} 16\pi\alpha_s(Q^2) f_{0^-}^2\, w_{0^-}^2(Q^2), \tag{1}$$

where: f_{0^-} is the meson's leptonic decay constant; $\alpha_s(Q^2)$ is the leading-order strong running-coupling

$$\alpha_s(Q^2) = 4\pi/[\beta_0\, \ln(Q^2/\Lambda_{\rm QCD}^2)], \tag{2}$$

with $\beta_0 = 11 - (2/3)n_f$ [n_f is the number of active quark flavours]; and

$$w_{0^-}(Q^2) = \frac{1}{3}\int_0^1 dx\, \frac{1}{x}\, \varphi_{0^-}(x;Q^2)\,, \tag{3}$$

where $\varphi_{0^-}(x;Q^2)$ is the meson's dressed-valence-quark distribution amplitude [DA]. This DA is determined by the meson's light-front wave function and relates to the probability that, with constituents collinear up to the scale $\zeta = \sqrt{Q^2}$, a valence-quark within the meson carries light-front fraction x of the bound-state's total momentum. Here, $\Lambda_{\rm QCD} \sim 0.2\,\mathrm{GeV}$ is the empirical mass-scale of QCD.

Crucially, the value of Q_0 is not predicted by perturbative QCD; but a hope that this scale might be as low as the proton mass, m_p, was influential in ensuring that the continuous electron beam accelerator facility [CEBAF] was planned with a peak beam energy of 4 GeV.

Before CEBAF began operations in 1994, little was known about the charged-pion electromagnetic form factor, $F_\pi(Q^2)$. A sound measurement of the pion's charge radius had been achieved by scattering high-energy pions from atomic electrons [5–8]. However, owing to kinematic limitations on the energy of the pion beam and unfavorable momentum transfer, different methods are required to reach higher Q^2. Electroproduction of pions from the nucleon can serve this purpose and precise data had been obtained at $Q^2/\mathrm{GeV}^2 = 0.35, 0.7$ [9–11]; but it was not until 1997 that a long-planned CEBAF experiment using this method collected data on $0.6 \leq Q^2/\mathrm{GeV}^2 \leq 1.6$ [12]. Analyses of subsequent experiments, which reached $Q^2 = 2.45\,\mathrm{GeV}^2$ by capitalising on higher beam energies available at a CEBAF exceeding original expectations, are described in Refs. [13–16]. However, no signal for the behaviour in Eq. (1) has yet been claimed. Consequently, experiments planned and approved at the upgraded Jefferson Lab [JLab 12] aim for precision measurements of $F_\pi(Q^2)$ to $Q^2 = 6\,\mathrm{GeV}^2$ and have the potential to reach $Q^2 \approx 8.5\,\mathrm{GeV}^2$ [17–19].

Eq. (1) involves the meson's DA, which is an essentially nonperturbative quantity. Lacking reliable predictions for the pointwise form of $\varphi_\pi(x;Q^2)$ appropriate to existing experimental scales, original expectations for empirical values of $Q^2F_\pi(Q^2)$ that would confirm Eq. (1) were based on the asymptotic profile [2–4]

$$\varphi_\pi(x;Q^2) \overset{\Lambda_{\rm QCD}^2/Q^2\simeq 0}{\approx} \varphi_\infty(x) = 6x(1-x)\,, \tag{4}$$

in which case

$$Q^2 F_\pi(Q^2) \overset{Q^2=4\,\mathrm{GeV}^2}{\approx} 0.15\,. \tag{5}$$

This prediction is a factor of 2.7 smaller than the empirical value quoted at $Q^2 = 2.45\,\mathrm{GeV}^2$ [15]: $0.41^{+0.04}_{-0.03}$.

Recently, however, continuum and lattice-QCD [lQCD] studies of the pseudoscalar meson bound-state problem have revealed that $\varphi_\pi(x;Q^2 \sim (2m_p)^2)$ is a concave function, much broader than φ_∞ owing to emergent mass generation in the Standard Model [20–29]. Using this information, a continuum calculation of $F_\pi(Q^2)$ on a large domain of spacelike momenta predicted [30] that the approved JLab 12 experiments [17, 31] are capable of validating Eq. (1) because the estimate in Eq. (5) is too small by a factor of approximately two.

lQCD validation of this prediction would be welcome. However, owing to competing demands [*e.g.* large lattice volume to represent light pions, small lattice spacing to reach large Q^2, and high statistics to compensate for decaying signal-to-noise ratio as form factors drop rapidly

* leichang@nankai.edu.cn
† cdroberts@anl.gov

with increasing Q^2], lQCD results with pion masses near the physical value, m_π, are currently restricted to small-Q^2: $0 < Q^2 \lesssim 0.25\,\mathrm{GeV}^2$ [32, 33]. Such analyses provide information about the pion's charge radius, but do not address the questions of whether and at which scale Eq. (1) is empirically applicable. No lQCD predictions at m_π are available on the full domain accessible to JLab 12, but new results exist on $Q^2 \lesssim 6\,\mathrm{GeV}^2$ at bound-state mass-squared values $m_{0^-}^2 \approx 10 m_\pi^2, 25 m_\pi^2$ [34, 35]. Herein, employing the continuum approach to the QCD bound-state problem that was used [30] to calculate the pion form factor and reconcile its behaviour with Eq. (1), we discuss how these modern lQCD results bear on validation of this hard scattering formula and related issues.

2. Computing pseudoscalar meson form factors. At leading order in the systematic, symmetry-preserving Dyson-Schwinger equation [DSE] approximation scheme described in Refs. [36–38], *viz.* rainbow-ladder [RL] truncation, the elastic form factor of a pion-like system constituted from degenerate current-quarks is given by [39–43]

$$K_\mu F_{0^-}(Q^2) = N_c \mathrm{tr} \int \frac{d^4k}{(2\pi)^4}\, \chi_\mu(k+p_f, k+p_i) \times \Gamma_{0^-}(k_i; p_i)\, S(k)\, \Gamma_{0^-}(k_f; -p_f)\,, \quad (6)$$

where Q is the incoming photon momentum, $p_{f,i} = K \pm Q/2$, $k_{f,i} = k + p_{f,i}/2$, $p_{f,i}^2 = -m_{0^-}^2$, and the trace is over spinor indices. The other elements in Eq. (6) are the dressed-quark propagator, $S(p)$, which, consistent with Eq. (6), is computed with the rainbow-truncation gap equation; and the 0^--meson Bethe-Salpeter amplitude $\Gamma_{0^-}(k;P)$ and unamputated dressed-quark-photon vertex, $\chi_\mu(k_f, k_i)$, both computed in RL truncation. [The impact of corrections to the RL computation is understood [44, 45]. The dominant effect is a modification of the power associated with the logarithmic running in Eq. (1). That running is slow and immaterial to the present discussion; but its effect can readily be incorporated when important.]

The leading-order DSE result for the pseudoscalar meson form factor is now determined once an interaction kernel is specified for the RL Bethe-Salpeter equation. We use that explained in Ref. [46, 47]:

$$\mathcal{K}_{\alpha_1\alpha_1',\alpha_2\alpha_2'} = \mathcal{G}_{\mu\nu}(k) [i\gamma_\mu]_{\alpha_1\alpha_1'} [i\gamma_\nu]_{\alpha_2\alpha_2'}\,, \quad (7a)$$

$$\mathcal{G}_{\mu\nu}(k) = \tilde{\mathcal{G}}(k^2) T_{\mu\nu}(k)\,, \quad (7b)$$

with $k^2 T_{\mu\nu}(k) = k^2 \delta_{\mu\nu} - k_\mu k_\nu$ and $(s = k^2)$

$$\tfrac{1}{Z_2^2}\tilde{\mathcal{G}}(s) = \frac{8\pi^2}{\omega^4} D e^{-s/\omega^2} + \frac{8\pi^2 \gamma_m \mathcal{F}(s)}{\ln\left[\tau + (1 + s/\Lambda_{\mathrm{QCD}}^2)^2\right]}\,, \quad (8)$$

where $\gamma_m = 4/\beta_0$, $\Lambda_{\mathrm{QCD}} = 0.234\,\mathrm{GeV}$, $\tau = \mathrm{e}^2 - 1$, and $\mathcal{F}(s) = \{1 - \exp(-s/[4m_t^2])\}/s$, $m_t = 0.5\,\mathrm{GeV}$. Z_2 is the dressed-quark wave function renormalisation constant. We employ a mass-independent momentum-subtraction renormalisation scheme for the gap and inhomogeneous vertex equations, implemented by making use of the scalar Ward-Green-Takahashi identity and fixing all renormalisation constants in the chiral limit [48], with renormalisation scale $\zeta = 2\,\mathrm{GeV} =: \zeta_2$.

The development of Eqs. (7), (8) is summarised in Ref. [46] and their connection with QCD is described in Ref. [49]; but it is worth reiterating some points. For instance, the interaction is deliberately consistent with that determined in studies of QCD's gauge sector, which indicate that the gluon propagator is a bounded, regular function of spacelike momenta that achieves its maximum value on this domain at $s = 0$ [49–58], and the dressed-quark-gluon vertex does not possess any structure which can qualitatively alter these features [59–67]. It is specified in Landau gauge because, *e.g.* this gauge is a fixed point of the renormalisation group and ensures that sensitivity to differences between *Ansätze* for the gluon-quark vertex are least noticeable, thus providing the conditions for which rainbow-ladder truncation is most accurate. The interaction also preserves the one-loop renormalisation group behaviour of QCD so that, *e.g.* the quark mass-functions produced are independent of the renormalisation point. On the other hand, in the infrared, *i.e.* $s \lesssim m_p^2$, Eq. (8) defines a two-parameter model, the details of which determine whether confinement and/or dynamical chiral symmetry breaking [DCSB] are realised in solutions of the dressed-quark gap equations.

Computations [46, 47] reveal that many properties of light-quark ground-state vector- and isospin-nonzero pseudoscalar-mesons are practically insensitive to variations of $\omega \in [0.4, 0.6]\,\mathrm{GeV}$, so long as

$$\varsigma^3 := D\omega = \text{constant}. \quad (9)$$

This feature also extends to numerous characteristics of the nucleon and Δ-baryon [68, 69]. The value of ς is chosen to reproduce, as well as possible, the measured value of the pion's mass and leptonic decay constant; and in RL truncation this requires

$$\varsigma = 0.82\,\mathrm{GeV}\,, \quad (10)$$

with renormalisation-group-invariant current-quark mass

$$\hat{m}_u = \hat{m}_d = \hat{m} = 6.6\,\mathrm{MeV}\,, \quad (11)$$

which corresponds to a one-loop evolved mass of $m^{\zeta_2} = 4.6\,\mathrm{MeV}$. We will subsequently employ $\omega = 0.5\,\mathrm{GeV}$, the midpoint of the insensitivity domain, and typically report the response of results to a 20% variation in this value.

The RL approximation to the elastic electromagnetic form factor of a pion-like pseudoscalar meson with mass m_{0^-} is now obtained as follows. (i) Perform a coupled solution of the dressed-quark gap- and meson Bethe-Salpeter-equations, defined via Eqs. (7), (8), varying the gap equation's current-quark mass until the Bethe-Salpeter equation has a solution at $P^2 = -m_{0^-}^2$, following Ref. [72] and adapting the algorithm improvements from Ref. [73] when necessary. (ii) With the dressed-quark propagator obtained thereby and the same interaction, solve the inhomogeneous Bethe-Salpeter equation

TABLE I. Input current-quark masses [one-loop evolved from an associated value of $\hat{m}$] for four pion-like mesons and related results computed with $\omega = 0.5\pm0.1$ GeV in Eqs. (8)-(10). $\langle\xi^2\rangle$, α are defined in Eqs. (12), (13). Empirically [70]: $f_\pi = 0.092\,$GeV, $r_\pi = 0.672(8)\,$fm. Regarding Row 2, the lQCD results at $m_{0^-} = 0.47\,$GeV [34] are associated with $f_{0^-} = 0.111(2)\,GeV$ [71], $r_{0^-} = 0.56(1)\,$fm [our estimate, using monopole fit to lattice results]; and concerning Row 3, Ref. [35] reports $f_{0^-} = 0.128\,$GeV, $r_{0^-} = 0.498(4)\,$fm for $m_{0^-} = 0.69\,$GeV. [In the table, all dimensioned quantities listed in GeV, except r_{0^-}, in fm.]

m^{ζ_2}	m_{0^-}	$\omega = 0.4$				$\omega = 0.5$				$\omega = 0.6$			
		f_{0^-}	r_{0^-}	$\langle\xi^2\rangle$	α	f_{0^-}	r_{0^-}	$\langle\xi^2\rangle$	α	f_{0^-}	r_{0^-}	$\langle\xi^2\rangle$	α
0.0046	0.14	0.092	0.63	0.255	0.46	0.094	0.66	0.265	0.39	0.097	0.68	0.273	0.33
0.053	0.47	0.115	0.53	0.217	0.80	0.115	0.55	0.226	0.71	0.115	0.56	0.229	0.68
0.107	0.69	0.135	0.47	0.196	1.05	0.133	0.49	0.207	0.92	0.133	0.49	0.211	0.87
0.152	0.83	0.147	0.43	0.180	1.28	0.145	0.45	0.193	1.09	0.145	0.45	0.200	1.00

to obtain the unamputated dressed-quark-photon vertex, including its dependence on Q^2, as described, *e.g.* in Ref. [74]. (iii) Combine these elements to form the integrand in Eq. (6) and compute the integral as a function of Q^2 to extract the form factor, $F_{0^-}(Q^2)$; an exercise first completed in Ref. [41].

To connect the results thus obtained and Eq. (1), the associated meson PDA at the same renormalisation scale is needed. It can be obtained from the meson's Poincaré-covariant Bethe-Salpeter amplitude following the methods described in Refs. [24–26, 75]. Namely, one computes the leading non-trivial Mellin moment of the PDA via

$$n\cdot P f_{0^-}\langle\xi^2\rangle = 3\,\mathrm{tr} Z_2 \int \frac{d^4k}{(2\pi)^4}\left[\frac{2n\cdot k}{n\cdot P}\right]^2 \times \gamma_5\gamma\cdot n\, S(k+P/2)\Gamma_{0^-}(k;P)S(k-P/2)\,, \quad (12)$$

with $\xi = (2x-1)$, $P^2 = -m_{0^-}^2$, $n^2 = 0$, $n\cdot P = -m_{0^-}$, using the same Poincaré-covariant regularisation of the integral as in the bound-state equations. A convergence-factor $1/[1+k^2r^2]$ is included in the integrand to stabilise the computation; the moment is computed as a function of r^2; and the final value is obtained by extrapolation to $r^2 = 0$. This procedure is efficient and reliable [75]. Using this moment, which is 1/5 when evaluated with φ_∞, one can reconstruct a realistic approximation to the PDA by writing

$$\varphi_{0^-}(x;\zeta_2) = x^\alpha(1-x)^\alpha\,\Gamma(2[\alpha+1])/\Gamma(\alpha+1)^2\,, \quad (13)$$

with α chosen to reproduce the calculated value of ξ^2. [The error in this procedure is negligible compared with that deriving from a 20% variation of ω in Eq. (9).]

3. Results. We have computed the form factors of pion-like mesons at four current-quark masses, corresponding to the physical pion, the lQCD meson masses in Refs. [34, 35], and one larger value, obtained by choosing the next evenly-spaced increment in current-quark mass. The results are reported in Table I and Fig. 1.

We approached the task without sophistication, using numerical solutions of the relevant gap and Bethe-Salpeter equations to directly evaluate the integral in Eq. (6). Owing to the analytic structure of some of the functions involved [72, 76], this algorithm fails on $Q^2 \gtrsim Q_f^2$, where $Q_f^2/\mathrm{GeV}^2 = 4,5,6,7$, respectively, for each row in Table I. Ref. [30] solved this problem by using perturbation theory integral representations [PTIRs] [77] for each matrix-valued function in Eq. (6), enabling a reliable computation of the electromagnetic form factor to arbitrarily large-Q^2. Constructing accurate PTIRs is, however, time consuming; and especially so here because one would need to build new PTIRs for each function at every one of the four current-quark masses. In completing the panels in Fig. 1 we therefore adapted the procedure introduced in Ref. [78], assuming that on the displayed domain each form factor can be expressed as

$$F_{0^-}(Q^2) = \frac{1}{1+Q^2/m_V^2}\mathcal{A}_{0^-}(Q^2)\,, \quad (14a)$$

$$\mathcal{A}_{0^-}(Q^2) = \frac{1+a_1Q^2+a_2^2Q^4}{1+Q^4(a_2^2/b_u^2)\ln[1+Q^2/\Lambda_{\mathrm{QCD}}^2]}\,, \quad (14b)$$

where m_V is the appropriate, computed vector meson mass and a_1, a_2, b_u are determined via a least-squares fit to the computed results on $Q^2 \leq Q_f^2$. The $\omega = 0.5\,$GeV values are (masses in GeV, coefficients in GeV^{-2})

m_{0^-}	m_V	a_1	a_2	b_u
0.14	0.77	−0.14	0.50	2.12
0.47	0.93	−0.16	0.54	2.00
0.69	1.10	−0.22	0.68	1.94
0.83	1.21	−0.22	0.81	1.89

(15)

(Empirical values for m_V/GeV in rows 1 and 3 are [70]: 0.775, 1.02.)

We validated this approach by using it to reanalyse the physical-pion results in Ref. [30]. This is the most challenging case because it requires extrapolation from $Q^2 = 4\,\mathrm{GeV}^2 \to 10\,\mathrm{GeV}^2$ to complete a curve on the domain depicted in Fig. 1A. Selecting only $Q^2 \leq 4\mathrm{GeV}^2$ results from Ref. [30], then, on the domain depicted, the obtained extrapolation function and the direct PTIR result are indistinguishable within any sensible measure of parameter sensitivity. (We used ±5% at $Q^2 = 10\,\mathrm{GeV}^2$.)

The results in Fig. 1A confirm the analysis in Ref. [30]. Namely, the calculated $F_\pi(Q^2)$ agrees semiquantitatively with the prediction of the hard-scattering formula,

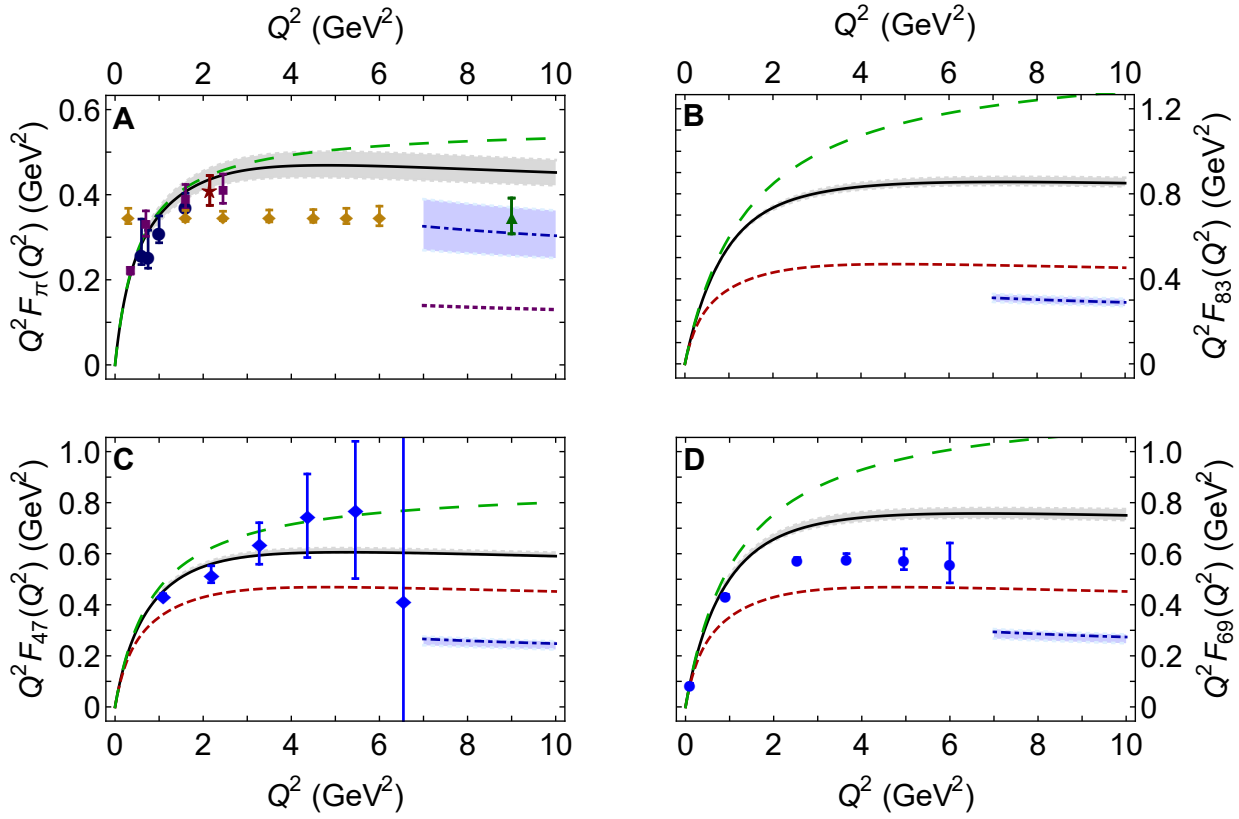

FIG. 1. Elastic form factors of pion-like pseudoscalar mesons. **A** – physical pion, $m_\pi = 0.14\,$GeV; **B** – mass-degenerate quarks, meson mass = 0.83 GeV; **C** – meson mass = 0.47 GeV; and **D** – meson mass = 0.69 GeV. Curves in each panel. Solid black curve within grey bands – our prediction: obtained with $w = 0.5 \pm 0.1\,$GeV in Eq. (8); long-dashed green curve – single-pole vector meson dominance result obtained with vector meson mass, m_V, computed consistent with the form factor prediction [see Eq. (15)]; and dot-dashed blue curve within blue bands – result from hard-scattering formula, Eq. (1), computed with the consistent meson decay constant and PDA. **A**. Dotted purple curve – Eq. (1) computed with the consistent pion decay constant and asymptotic DA, $\varphi_\infty(x) = 6x(1-x)$; filled-circles and -squares – data described in Ref. [15]; and filled gold diamonds and green triangle – projected reach and accuracy of forthcoming experiments [18, 79]. For comparison, the dashed red curve in the other panels is the black curve from **A**, *viz.* the physical-pion form factor prediction. **C** – filled blue diamonds, lQCD results in Ref. [34]; and **D** – filled blue circles, lQCD results in Ref. [35].

Eq. (1), when the PDA appropriate to the empirical scale is used. The difference between these two curves is explained by a combination of higher-order, higher-twist corrections to Eq. (1) on the one hand and, on the other, shortcomings in the rainbow-ladder truncation, described above. Hence, as explained in Ref. [30], one should expect dominance of hard contributions to the pion form factor for $Q^2 \gtrsim 8\,$GeV^2. Notwithstanding this, the normalisation of the form factor is fixed by a pion wave-function whose dilation with respect to $\varphi_\infty(x)$ is a definitive signature of DCSB.

In addition to the preceding observations, the panels in Fig. 1 expose numerous features relating to the evolution of these elastic form factors with meson mass.

(i) The charge radius decreases with increasing mass, *i.e.* the bound-states become more pointlike; and $r_{0^-} \propto 1/f_{0^-}$, up to $\ln m_{0^-}$-corrections. This is illustrated in Fig. 2A and explained elsewhere [80].

r_{0^-} is an intrinsic length-scale in these systems. The meson becomes a more highly correlated state as it diminishes. Hence, steadily increasing values of Q^2 are required to reach the domain upon which Eq. (1) provides a useful guide to $F_{0^-}(Q^2)$.

(ii) This last feature is readily apparent in Fig. 1. Proceeding anticlockwise from **A** → **C** → **D** → **B**, the mismatch increases between the direct calculation [solid black curve] and the result obtained using Eq. (1) with the appropriate f_{0^-}, $\varphi_{0^-}(x;Q^2)$ [dot-dashed blue curve].

(iii) The failure of the Eq. (1) prediction to increase in magnitude as quickly as the direct calculation is explained by a feature of the meson PDA's $\langle 1/x\rangle$-moment, illustrated in Fig. 2B. Namely, $f_{0^-} w_{0^-}$ is roughly constant on the domain of meson masses considered: with $\omega = 0.5\,$GeV, the integrated relative difference between the computed m_{0^-}-dependence and the mean value is just 3%. Conse-

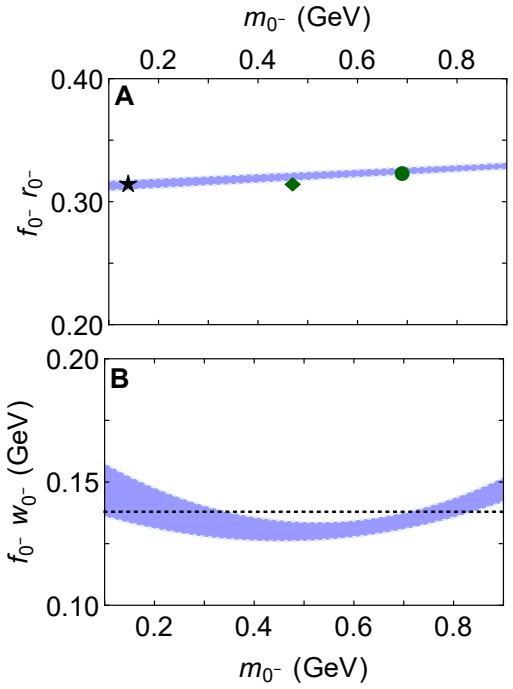

FIG. 2. **A**. $f_{0^-} r_{0^-}$ as a function of meson mass. It is nearly constant over a large range [80, 81]. Black star – empirical value for the pion; green diamond – lQCD [34]; and green circle – lQCD [35]. **B**. $f_{0^-} w_{0^-}$: w_{0^-} is the $\langle 1/x \rangle$-moment in Eq. (3). This function takes a minimum value in the neighbourhood of the s-quark current-mass and then evolves toward linear growth with m_{0^-}, up to logarithmic corrections. The dotted black line marks the mean value. The bands in both panels describe the range of results obtained for $\omega \in [0.4, 0.6]$ GeV.

quently, the prediction of the hard-scattering formula is weakly varying on $m_{0^-} \in [0.1, 0.9]$ GeV, whereas the form factor itself rises steadily with m_{0^-}, owing primarily to the decreasing radius [increasing f_{0^-}] of the system.

Evidently, therefore, the growing Higgs-generated current-quark mass drives away the domain whereupon the exclusive hard-scattering formula is applicable for the associated bound-state. This property, *viz.* that with growing mass, increasingly larger values of Q_0^2 are required in order to enter the domain of validity for hard-scattering formulae, is also found in the treatment of $\gamma\gamma^* \to$ neutral-0^--meson transition form factors [45].

It is worth noting, too, that the minimum of the $f_{0^-} w_{0^-}$ curve occurs in the neighbourhood of the s-quark current-mass. This is a consequence of the fact, shown elsewhere [82] and evident from the values of α_{0^-} in Table I, that $\varphi_{0^-}(x; Q^2) \approx \varphi_\infty(x)$ in this neighbourhood. With masses increasing away from this domain, $f_{0^-} w_{0^-}$ becomes a linear function, up to $\ln m_{0^-}$-corrections.

(iv) Notwithstanding these facts, the direct calculation's deviation from the trajectory defined by the single-pole vector-meson-dominance [VMD] prediction [long-dashed green curve] also increases with m_{0^-}, and in each case the departure begins at a steadily decreasing value of Q^2. These effects owe to a shift to deeper timelike values of the ground-state vector-meson mass, so that this resonance contribution to the dressed-quark-photon vertex diminishes in importance for the meson-photon coupling, and parallel alterations in the pseudoscalar meson's internal structure. Such deviation from the VMD prediction is a crucial prerequisite to entering the validity domain of Eq. (1).

Comparing Figs. 1C, 1D, it seems that the lQCD results in Refs. [34, 35] are mutually inconsistent: the lighter meson mass in Ref. [34] is associated with an elastic form factor which is larger in magnitude than that describing the internal structure of the heavier 0^{-+}-meson in Ref. [35]. We have insufficient information to resolve this issue; but can observe that whilst the low-scale results from both studies match our predictions, only Ref. [34] is consistent with our calculations on the domain of larger-Q^2.

4. Summary and Conclusions. We employed the leading-order approximation in a symmetry-preserving, continuum analysis of the quark-antiquark bound-state problem to determine electromagnetic form factors of pion-like mesons with masses $m_{0^-}/\text{GeV} = 0.14, 0.47, 0.69, 0.83$ on a spacelike domain that extends to $Q^2 \lesssim 10\,\text{GeV}^2$; and simultaneously computed the parton distribution amplitudes of each system. The results exposed an array of novel features, with relevance to experiment and also *ab initio* lattice-QCD studies of these systems. Of particular significance is the conclusion that the form factor of the physical pion provides the best opportunity for verification of the leading-order, leading-twist factorised hard-scattering formula for such exclusive processes. This is because the lower bound, Q_0, of the domain upon which that formula is valid increases quickly with growing m_{0^-}, *i.e.* more generally, the inflating mass-scale introduced by increasing Higgs-generated current-quark masses drives away the domain whereupon any relevant exclusive hard-scattering formula is applicable for the associated bound-state.

Acknowledgments. We are grateful for insightful comments from S. J. Brodsky, R. Ent, T. Horn, A. Lovato and J. Zanotti. Work supported by: the Chinese Government's Thousand Talents Plan for Young Professionals; the Chinese Ministry of Education, under the *International Distinguished Professor* programme; and U.S. Department of Energy, Office of Science, Office of Nuclear Physics, under contract no. DE-AC02-06CH11357.

[1] G. R. Farrar and D. R. Jackson, Phys. Rev. Lett. **43**, 246 (1979).
[2] G. P. Lepage and S. J. Brodsky, Phys. Lett. B **87**, 359 (1979).
[3] A. V. Efremov and A. V. Radyushkin, Phys. Lett. B **94**, 245 (1980).
[4] G. P. Lepage and S. J. Brodsky, Phys. Rev. D **22**, 2157 (1980).
[5] E. B. Dally *et al.*, Phys. Rev. D **24**, 1718 (1981).
[6] E. B. Dally *et al.*, Phys. Rev. Lett. **48**, 375 (1982).
[7] S. R. Amendolia *et al.*, Phys. Lett. B **146**, 116 (1984).
[8] S. R. Amendolia *et al.*, Nucl. Phys. B **277**, 168 (1986).
[9] H. Ackermann *et al.*, Nucl. Phys B. **137**, 294 (1978).
[10] P. Brauel *et al.*, Phys. Lett. B **69**, 253 (1977).
[11] P. Brauel *et al.*, Z. Phys C **3**, 101 (1979).
[12] J. Volmer *et al.*, Phys. Rev. Lett. **86**, 1713 (2001).
[13] T. Horn *et al.*, Phys. Rev. Lett. **97**, 192001 (2006).
[14] T. Horn *et al.*, Phys. Rev. C **78**, 058201 (2008).
[15] G. Huber *et al.*, Phys. Rev. C **78**, 045203 (2008).
[16] H. P. Blok *et al.*, Phys. Rev. C **78**, 045202 (2008).
[17] Huber, G. M., Gaskell, D. *et al.*, *Measurement of the Charged Pion Form Factor to High Q^2*, approved Jefferson Lab 12 GeV Experiment E12-06-101, 2006.
[18] Horn, T., Huber, G. M. *et al.*, *Scaling Study of the L/T-Separated Pion Electroproduction Cross Section at 11 GeV*, approved Jefferson Lab 12 GeV Experiment E12-07-105, 2007.
[19] T. Horn, EPJ Web Conf. **137**, 05005 (2017).
[20] S. Mikhailov and A. Radyushkin, JETP Lett. **43**, 712 (1986).
[21] V. Y. Petrov, M. V. Polyakov, R. Ruskov, C. Weiss and K. Goeke, Phys. Rev. D **59**, 114018 (1999).
[22] S. J. Brodsky and G. F. de Teramond, Phys. Rev. Lett. **96**, 201601 (2006).
[23] R. Arthur *et al.*, Phys. Rev. D **83**, 074505 (2011).
[24] L. Chang *et al.*, Phys. Rev. Lett. **110**, 132001 (2013).
[25] I. C. Cloët, L. Chang, C. D. Roberts, S. M. Schmidt and P. C. Tandy, Phys. Rev. Lett. **111**, 092001 (2013).
[26] J. Segovia *et al.*, Phys. Lett. B **731**, 13 (2014).
[27] V. M. Braun *et al.*, Phys. Rev. D **92**, 014504 (2015).
[28] T. Horn and C. D. Roberts, J. Phys. G. **43**, 073001 (2016).
[29] J.-H. Zhang, J.-W. Chen, X. Ji, L. Jin and H.-W. Lin, Phys. Rev. D **95**, 094514 (2017).
[30] L. Chang, I. C. Cloët, C. D. Roberts, S. M. Schmidt and P. C. Tandy, Phys. Rev. Lett. **111**, 141802 (2013).
[31] T. Horn and G. M. Huber, (2007), Jefferson Lab Experiment E12-07-105.
[32] J. Koponen, F. Bursa, C. T. H. Davies, R. J. Dowdall and G. P. Lepage, Phys. Rev. D **93**, 054503 (2016).
[33] C. Alexandrou *et al.*, Phys. Rev. D **97**, 014508 (2018).
[34] A. J. Chambers *et al.*, Phys. Rev. D **96**, 114509 (2017).
[35] J. Koponen, A. C. Zimermmane-Santos, C. T. H. Davies, G. P. Lepage and A. T. Lytle, Phys. Rev. D **96**, 054501 (2017).
[36] H. J. Munczek, Phys. Rev. D **52**, 4736 (1995).
[37] A. Bender, C. D. Roberts and L. von Smekal, Phys. Lett. B **380**, 7 (1996).
[38] C. D. Roberts, (nucl-th/9609039), *Confinement, diquarks and Goldstone's theorem*.
[39] C. D. Roberts, Nucl. Phys. A **605**, 475 (1996).
[40] P. Maris and C. D. Roberts, Phys. Rev. C **58**, 3659 (1998).
[41] P. Maris and P. C. Tandy, Phys. Rev. C **62**, 055204 (2000).
[42] A. Höll, A. Krassnigg, P. Maris, C. D. Roberts and S. V. Wright, Phys. Rev. C **71**, 065204 (2005).
[43] M. S. Bhagwat and P. Maris, Phys. Rev. C **77**, 025203 (2008).
[44] K. Raya *et al.*, Phys. Rev. D **93**, 074017 (2016).
[45] K. Raya, M. Ding, A. Bashir, L. Chang and C. D. Roberts, Phys. Rev. D **95**, 074014 (2017).
[46] S.-X. Qin, L. Chang, Y.-X. Liu, C. D. Roberts and D. J. Wilson, Phys. Rev. C **84**, 042202(R) (2011).
[47] S.-X. Qin, L. Chang, Y.-X. Liu, C. D. Roberts and D. J. Wilson, Phys. Rev. C **85**, 035202 (2012).
[48] L. Chang *et al.*, Phys. Rev. C **79**, 035209 (2009).
[49] D. Binosi, L. Chang, J. Papavassiliou and C. D. Roberts, Phys. Lett. B **742**, 183 (2015).
[50] P. O. Bowman *et al.*, Phys. Rev. D **70**, 034509 (2004).
[51] P. Boucaud *et al.*, JHEP **06**, 001 (2006).
[52] P. Boucaud *et al.*, Few Body Syst. **53**, 387 (2012).
[53] A. Ayala, A. Bashir, D. Binosi, M. Cristoforetti and J. Rodríguez-Quintero, Phys. Rev. D **86**, 074512 (2012).
[54] A. Aguilar, D. Binosi and J. Papavassiliou, Phys. Rev. D **86**, 014032 (2012).
[55] D. Binosi, C. D. Roberts and J. Rodríguez-Quintero, Phys. Rev. D **95**, 114009 (2017).
[56] D. Binosi, C. Mezrag, J. Papavassiliou, C. D. Roberts and J. Rodríguez-Quintero, Phys. Rev. D **96**, 054026 (2017).
[57] F. Gao, S.-X. Qin, C. D. Roberts and J. Rodriguez-Quintero, Phys. Rev. D **97**, 034010 (2018).
[58] J. Rodríguez-Quintero, D. Binosi, C. Mezrag, J. Papavassiliou and C. D. Roberts, Few Body Syst. **59**, 121 (2018).
[59] J. I. Skullerud, P. O. Bowman, A. Kızılersü, D. B. Leinweber and A. G. Williams, JHEP **04**, 047 (2003).
[60] M. S. Bhagwat and P. C. Tandy, Phys. Rev. D **70**, 094039 (2004).
[61] A. C. Aguilar, D. Binosi, D. Ibañez and J. Papavassiliou, Phys. Rev. D **90**, 065027 (2014).
[62] R. Williams, C. S. Fischer and W. Heupel, Phys. Rev. D **93**, 034026 (2016).
[63] D. Binosi, L. Chang, S.-X. Qin, J. Papavassiliou and C. D. Roberts, Phys. Rev. D **93**, 096010 (2016).
[64] D. Binosi, L. Chang, J. Papavassiliou, S.-X. Qin and C. D. Roberts, Phys. Rev. D **95**, 031501(R) (2017).
[65] A. C. Aguilar, J. C. Cardona, M. N. Ferreira and J. Papavassiliou, Phys. Rev. D **96**, 014029 (2017).
[66] R. Bermudez, L. Albino, L. X. Gutiérrez-Guerrero, M. E. Tejeda-Yeomans and A. Bashir, Phys. Rev. D **95**, 034041 (2017).
[67] A. K. Cyrol, M. Mitter, J. M. Pawlowski and N. Strodthoff, Phys. Rev. D **97**, 054006 (2018).
[68] G. Eichmann, I. C. Cloët, R. Alkofer, A. Krassnigg and C. D. Roberts, Phys. Rev. C **79**, 012202(R) (2009).
[69] G. Eichmann, Prog. Part. Nucl. Phys. **67**, 234 (2012).
[70] C. Patrignani *et al.*, Chin. Phys. C **40**, 100001 (2016).
[71] V. G. Bornyakov *et al.*, Phys. Lett. B **767**, 366 (2017).
[72] P. Maris and C. D. Roberts, Phys. Rev. C **56**, 3369 (1997).
[73] A. Krassnigg, PoS **CONFINEMENT8**, 075 (2008).

[74] P. Maris and P. C. Tandy, Phys. Rev. C **61**, 045202 (2000).
[75] B. L. Li *et al.*, Phys. Rev. D **93**, 114033 (2016).
[76] A. Windisch, Phys. Rev. C **95**, 045204 (2017).
[77] N. Nakanishi, Prog. Theor. Phys. Suppl. **43**, 1 (1969).
[78] S.-X. Qin, C. Chen, C. Mezrag and C. D. Roberts, Phys. Rev. C **97**, 015203 (2018).
[79] Huber, G. M. and Gaskell, D. *et al.*, (2006), Jefferson Lab Experiment E12-06-101.
[80] M. S. Bhagwat, A. Krassnigg, P. Maris and C. D. Roberts, Eur. Phys. J. A **31**, 630 (2007).
[81] I. C. Cloët and C. D. Roberts, PoS **LC2008**, 047 (2008).
[82] M. Ding, F. Gao, L. Chang, Y.-X. Liu and C. D. Roberts, Phys. Lett. B **753**, 330 (2016).